

RESEARCH ARTICLE

10.1002/2016MS000846

On the role of the stratiform cloud scheme in the inter-model spread of cloud feedback

O. Geoffroy¹, S. C. Sherwood¹ , and D. Fuchs¹ 

¹Climate Change Research Centre, University of New South Wales, Sydney, New South Wales, Australia

Key Points:

- The stratiform cloud scheme plays an important role in the spread of cloud feedback, both in Sc regions and globally
- Subgrid PDF schemes tend to impose a positive low cloud feedback and stability dependence a negative feedback
- Stability dependence does not fully determine the sign of the feedback, including in marine stratus regions

Supporting Information:

- Supporting Information S1
- Figure S1
- Figure S2
- Figure S3
- Figure S4
- Figure S5
- Figure S6
- Figure S7
- Figure S8

Correspondence to:

O. Geoffroy,
o.geoffroy@unsw.edu.au

Citation:

Geoffroy, O., S. C. Sherwood, and D. Fuchs (2017), On the role of the stratiform cloud scheme in the inter-model spread of cloud feedback, *J. Adv. Model. Earth Syst.*, 9, 423–437, doi:10.1002/2016MS000846.

Received 28 OCT 2016

Accepted 5 JAN 2017

Accepted article online 10 JAN 2017

Published online 12 FEB 2017

© 2017. The Authors.

This is an open access article under the terms of the Creative Commons Attribution-NonCommercial-NoDerivs License, which permits use and distribution in any medium, provided the original work is properly cited, the use is non-commercial and no modifications or adaptations are made.

Abstract This study explores the role of the stratiform cloud scheme in the inter-model spread of cloud feedback. Six diagnostic cloud schemes used in various CMIP (Coupled Model Intercomparison Experiment) climate models are implemented (at low and midlevels) into two testbed climate models, and the impacts on cloud feedback are investigated. Results suggest that the choice of stratiform cloud scheme may contribute up to roughly half of the intermodel spread of cloud radiative responses in stratocumulus (Sc) regions, and may determine or favor a given sign of the feedback there. Cloud schemes assuming a probability density function for total water content consistently predict a positive feedback in Sc regions in our experiments. A large negative feedback in Sc regions is obtained only with schemes that consider variables other than relative humidity (e.g., stability). The stratiform cloud scheme also significantly affects cloud feedback at the scale of the tropics and at global scale. Results are slightly less consistent for tropical means, likely indicating coupling with other boundary layer processes such as convective mixing.

1. Introduction

The cloud radiative response to global warming, or cloud radiative feedback, in particular that contributed by tropical low clouds, has been identified as a major source of spread of climate sensitivity [Dufresne and Bony, 2008; Zelinka et al., 2016]. Understanding the sources of spread of such feedbacks is important for improving model physics, leading future climate model development priorities, and narrowing uncertainties in future climate projections. Parameterizations of the boundary layer and/or shallow convective processes have been shown to play an important role in this spread [Gettelman et al., 2012; Zhang et al., 2013, Sherwood et al., 2014, Webb et al., 2015]. The analysis of Qu et al. [2014] suggests a large role for cloud macrophysics (i.e., the representation of cloud cover) and turbulence parameterizations in the spread of low cloud feedback, which in turn is a dominant influence on global feedback. However, other studies point to the importance of convective physics in global climate sensitivity, for example, entrainment or precipitation efficiency rates [Stainforth et al., 2005; Zhao et al., 2016]. This raises the question of the relative roles of the low-cloud, convective, and other parameterizations in explaining the model spread.

If dry static stability alone controlled cloud amount, a warmer climate would have more low cloud [e.g., Bretherton et al., 2013]. However sea surface and free troposphere warming at constant relative humidity can oppose this, through thermodynamic mechanisms leading to a reduction of the cloud layer relative humidity [Rieck et al., 2012; Bretherton, 2015]. Qu et al. [2014] show that climate models employing a total water probability density function (PDF)-based low-cloud scheme predict low cloud cover (LCC) reduction in the stratocumulus (Sc) regions, whereas most models employing a scheme with a stability dependent cloud fraction predict an increase of LCC in the Sc regions. However, this relationship between the Sc-regions LCC response and parameterization type may be fortuitous, due to the limited number of models and parameterization type combinations of the CMIP ensemble, and the lack of independence between climate models.

In this study, we focus on the role of the stratiform cloud macrophysics and microphysics parameterizations in the CMIP inter-model spread of cloud feedback. We implement a range of stratiform cloud schemes (cloud fraction and cloud water content parameterizations) found in CMIP models into two testbed models, CAM4 [Neale et al., 2010] and CSIRO-Mk3L [Gordon et al., 2002; Phipps et al., 2011], and assess their impact on cloud responses. Section 2 describes the models used, the cloud schemes implemented, and the experiments performed. The results are presented in section 3. Final discussion and conclusions are drawn in section 4.

Table 1. Summary of the Climate Models Used in This Study, Their Stratiform Cloud Scheme Type and the Type of Simulations Used to Estimate Their Cloud Responses

Model	CMIP	Cloud Scheme	Model and Cloud Scheme References	Responses Estimated From
ACCESS1-3	5	A1	<i>Martin et al.</i> [2011], <i>Smith</i> [1990]	abrupt4xCO2 (regression)
HadGEM2-ES	5	A1	<i>Martin et al.</i> [2011], <i>Smith</i> [1990]	AMIP, AMIP4K
CSIRO-Mk3.6.0	5	A1	<i>Rotstayn et al.</i> [2010], <i>Rotstayn</i> [1997], <i>Smith</i> [1990]	abrupt4xCO2 (regression)
CSIRO-Mk3L	/	A1	<i>Phipps et al.</i> [2011], <i>Rotstayn</i> [1997], <i>Smith</i> [1990]	AMIP, AMIP4K
MIROC-ESM	5	A2	<i>Watanabe et al.</i> [2011], <i>Le Treut and Li</i> [1991]	abrupt4xCO2 (regression)
IPSL-CMA-LR	5	A3	<i>Dufresne et al.</i> [2013], <i>Hourdin et al.</i> [2006], <i>Bony and Emanuel</i> [2001]	AMIP, AMIP4K
CGCM3	3	B	<i>Scinocca et al.</i> [2008], <i>McFarlane et al.</i> [1992]	slabcntrl, 2xco2
INM-CM4	5	C	<i>Volodin et al.</i> [2010], <i>Volodin</i> [2014]	abrupt4xCO2 (regression)
BCC-CSM1-1	5	D	<i>Wu et al.</i> [2010], <i>Neale et al.</i> [2010]	AMIP, AMIP4K
CAM4	5	D	<i>Neale et al.</i> [2010]	AMIP, AMIP4K
FGOALS-g2	5	D	<i>Li et al.</i> [2013], <i>Neale et al.</i> [2010]	AMIP, AMIP4K
NorESM1-M	5	D	<i>Bentsen et al.</i> [2012], <i>Neale et al.</i> [2010]	AMIP, AMIP4K
PCM1	3	E1	<i>Washington et al.</i> [2000], <i>Kiehl et al.</i> [1996]	1pctto2xCO2 (last minus first years)
FGOALS-s2	5	E2	<i>Bao et al.</i> [2013], <i>Liu et al.</i> [1998], <i>Fushan et al.</i> [2005], <i>Xu and Randall</i> [1996]	abrupt4xCO2 (regression)

2. Methodology and Numerical Experiments

2.1. General Method and Models

We modify the original stratiform cloud schemes of both CAM4 and CSIRO-Mk3L, by implementing cloud parameterizations originating from others climate models of the CMIP ensemble. CAM4 is the atmospheric component of CESM climate model, described by *Neale et al.* [2010]. Here we use zonal and meridional resolutions respectively of 2.5° and 1.9° for CAM4, and 5.6° and 3.2° for CSIRO-Mk3L. In CAM4, deep and shallow convection schemes follow *Zhang and McFarlane* [1995] and *Hack* [1994], respectively. In CSIRO-Mk3L, the deep convection scheme follows *Gregory and Rowntree* [1990] and the model is run without shallow convection. Lastly, CSIRO-Mk3L uses the same turbulence scheme as CAM4, which in particular features a non-local atmospheric boundary layer scheme based on *Holtstlag and Moeng* [1991]. Stratiform cloud schemes of each model are described in the next subsection. The equilibrium climate sensitivities (ECS) of CSIRO-Mk3L and CCSM4 are roughly 3.4 K and 2.9 K [*Geoffroy et al.*, 2013], respectively.

The perturbation or replacement of the stratiform cloud scheme of a given model allows the effect of this scheme to be isolated in a way not possible with multimodel analyses. This perturbed physics ensemble, using two testbed models, is considered alongside the subset of CMIP models containing the considered cloud schemes, in order to situate the results in the broader context of the multimodel ensemble, and highlight the role of the cloud scheme in the ensemble spread of cloud feedback. For practical reasons, we consider only schemes having a diagnostic cloud fraction and, generally a diagnostic cloud water content, and which are not directly coupled to other parameterizations (such as turbulence and convection). For this reason, this study focuses on cloud schemes of a subset of climate models of the CMIP3 [*Meehl et al.*, 2007] and CMIP5 [*Taylor et al.*, 2012] ensemble. These schemes are grouped into five categories referred to as A, B, C, D and E as indicated, along with the associated CMIP models, in Table 1. These five cloud-scheme categories represent the schemes used in almost two thirds of the CMIP3 and CMIP5 climate models studied in *Qu et al.* [2014]. Note that for any cloud scheme used in both CMIP3 and CMIP5 models, only results from the CMIP5 model are shown. The next section provides a brief description of the cloud schemes, details being provided in the Appendix A.

2.2. Perturbed Cloud Schemes Description

Stratiform cloud scheme Category A represents the most common type used in CMIP models. We refer to schemes in this category as probability-density function (PDF) schemes. Cloud fraction and cloud water content are diagnosed from liquid temperature (or temperature) and total water content assuming a PDF for the subgrid distribution of the moisture [e.g., *Smith*, 1990]. Three subclasses can be considered, based on

(among other differences) the shape of PDF used. Category A1, A2 and A3 refer to *Le Treut and Li* [1991] (uniform distribution), *Smith* [1990] (triangular distribution) and *Bony and Emanuel* [2001] (Gaussian distribution) schemes, respectively. For each scheme, other particular specifications are provided in the Appendix A. CMIP3 models with Category A schemes (not shown) show similar cloud responses to CMIP5 models [Qu *et al.*, 2014]. The climate models used in our study are listed in Table 1.

The CSIRO-Mk3L stratiform cloud scheme belongs to Category A1. Note that in CSIRO-Mk3L, the threshold relative humidity (RH) varies in convective regions between cloud base and cloud top. This assumption is not made when implementing this scheme in CAM4. The CSIRO-Mk3L stratiform cloud scheme is based on *Rotstayn* [1997]: both water vapor and cloud water content are prognostic variables.

Category B represents the cloud scheme implemented in the CMIP3 model CGCM [Scinocca *et al.*, 2008]. Note that this scheme was also erroneously attributed to CanESM2 (CMIP5 model) by *Chylek et al.* [2011] and *Qu et al.* [2014] (J. Cole, personal communication, 2016, see also <http://ec.gc.ca/ccmac-cccma/default.asp?lang=En&n=8A6F8F67-1>). The cloud fraction depends on both RH and local stability. This stability dependence directly enters the cloud fraction formulation as an additional parameter, rather than being expressed in a separate Sc cloud scheme. For profiles less stable than the local moist adiabatic, cloud fraction is a function of RH only.

Category C represents the cloud scheme implemented in the CMIP5 model INM-CM4 [Volodin, 2014]: the cloud fraction is a linear function of RH with the coefficients varying with local stability, and the cloud water content is a function of temperature only.

Category D includes schemes that are implemented in climate models from which the atmospheric component (or the cloud scheme) are based on CAM3 or CAM4, which have identical cloud schemes [Collins *et al.*, 2004; Neale *et al.*, 2010]. In addition to the NCAR model CESM, the other CMIP5 models employing this scheme are BCC-CSM1.1 [Wu *et al.*, 2010] and NorESM [Bentsen *et al.*, 2012] and FGOALS-g2 [Li *et al.*, 2013]. In Category D models, the cloud fraction is a function of RH. Cloud fraction also depends on stability. In contrast to Categories B and C, this dependence on stability is expressed through a separate Sc scheme: when a marine stratocumulus is diagnosed (from local stability), its cloud fraction is a function of lower tropospheric stability (LTS). The cloud water content is prognostic and is related to temperature, water vapour and cloud water tendencies, cloud fraction and thermodynamical variables.

Subcategory E1 of category E denotes parameterizations based on the CCM3 scheme [Kiehl *et al.*, 1996]. This scheme is diagnostic and cloud fraction is expressed as a function of RH and both vertical velocity and stability. Note that in CCM3, the cloud water for cloud radiative properties differs from that used to diagnose stratiform precipitation. Here the former formulation is also used in the precipitation calculation. One other model of the CMIP ensemble (FGOALS-s2) has similar dependence of cloud fraction on vertical velocity. The FGOALS-s2 stratiform scheme is denoted E2. Note that FGOALS-s2 contains also a Sc scheme that is not implemented for E2.

In perturbed cloud-scheme experiments, both cloud fraction and cloud water content parameterizations are modified. The stratiform precipitation parameterization is kept as that of the original model. Moreover, in both CSIRO-Mk3L and CAM4, cloud water is split into liquid and ice according to temperature. These calculations of liquid and ice fraction are unchanged. Finally, the convective cloud fraction and its combination with stratiform cloud fraction to get the total cloud fraction at a given level are also unchanged.

2.3. Numerical Experiments

Cloud responses to global warming in CSIRO-Mk3L and CAM4 are determined by using AMIP and AMIP+4K experiments. Note that sea ice is unchanged in the AMIP+4K experiments for both models. Hence, CAM4 simulations analyzed in this study are not rigorously equivalent to CCSM4 simulations of the CMIP5 archive responses, but responses do not differ significantly. In addition to their low numerical cost, AMIP experiments exclude any tropospheric fast adjustment and enable a direct comparison between simulations with similar SST pattern. For each CMIP model, we use AMIP (fixed SST) and AMIP4K (fixed SST plus 4 K) when available (only in CMIP5). Otherwise, experiments used are, in preferential order of availability: the abrupt4xCO₂ (ocean coupled abrupt 4xCO₂) experiment (CMIP5); the slab (slab-ocean coupled control simulation) and 2xco2 (slab-ocean coupled simulation with CO₂ doubling) experiments (CMIP3), referred

hereafter as slab experiments; or the 1pctto2xCO₂ experiments (ocean coupled with 1% CO₂ increase per year to doubling followed by a stabilization; CMIP3).

In the case of the abrupt experiments, responses, of cloud fraction or cloud radiative effect CRE changes per unit of warming, are determined from a linear regression method [Gregory *et al.*, 2004] (regression of the considered variable change against the surface air temperature change, by using, for both variables, annual means over the considered region). The CRE is defined as the difference between all-sky and clear-sky net incoming (longwave plus shortwave) radiative fluxes at top of the atmosphere. Note that we have not used the control experiment to attempt to remove any potential drifts, as these have been found not to significantly affect estimates of the feedback parameter for CMIP5 models [Geoffroy *et al.*, 2013]. Responses estimated from AMIP and from abrupt4xCO₂ experiments show good agreement for the CMIP5 ensemble of models with both types of experiments available (not shown), in agreement with the results of Ringer *et al.* [2014]. For both AMIP type, slab type, and 1pctto2xCO₂, the responses are calculated by differencing 15 year means of the control and perturbed states (defined, for 1pctto2xCO₂, as the first years and the last years for the simulation, respectively). In particular, the forcing adjustment contribution is not removed for these estimates.

3. Results

3.1. Stratocumulus Regions

As a first step, the stratiform cloud scheme is modified in lower levels only, below 750 hPa. Note that the threshold 750 hPa was used as a limit for low cloud because it is the default separation-level used in CAM4 between low and midlevel clouds (we applied the same threshold with CSIRO-Mk3L). To evaluate the impact of model changes on the cloud feedback, we focus mainly on two variables: cloud radiative effect (CRE) and low cloud cover (LCC). The LCC is defined as the mean of the maximum (stratiform plus convective) cloud fraction below 700 hPa in each atmospheric column (the level was chosen slightly higher than that used to perturb cloud, because changes were seen to extend somewhat above 750 hPa). The CRE change is closely related to the cloud radiative feedback, although quantitatively different due to masking effects [Soden and Held, 2006]. By contrast, cloud cover changes allow us to distinguish cloud responses at different levels and highlight the sign of the cloud responses (under the assumption that cover changes dominate over, or are strongly correlated with, optical depth changes). Figure 1 shows mean LCC change and mean CRE in the stratocumulus (Sc) regions, and associated normalized changes by the value in the mean state, for both CMIP models and CAM4 and CSIRO-Mk3L perturbed experiments. Sc regions are defined as five rectangular regions of 20° latitude by 40° longitude in the eastern margins of tropical oceans, as in Qu *et al.* [2014].

The results show that a modification of the cloud scheme in the lower levels leads to a large range of responses for both LCC change and CRE change, highlighting the importance of the stratiform cloud parameterization for cloud feedback. As shown in Figure 2, changing the cloud scheme below 750 hPa only significantly impacts both cloud fraction and cloud fraction change in the lowest levels suggesting that the impact on global cloud feedback is associated with low level clouds response, and not with higher clouds. The standard deviations of the LCC response are 0.60% K⁻¹ and 0.26% K⁻¹ for CAM4 and CSIRO-Mk3L ensembles, respectively, against 0.81% K⁻¹ for the CMIP subensemble. Hence, the cloud scheme may explain up to roughly 50% of the CMIP subensemble spread of Sc-LCC changes (and 40% for the CRE). This value corresponds to the mean ratio of CAM4 and CSIRO-Mk3L ensembles standard deviations to CMIP subensemble standard deviation. Note that this rough estimate is only an upper bound because the cloud feedback dependencies to the cloud scheme are not systematically consistent. Note also that weighting the standard deviation calculation by the number of CMIP models in each cloud scheme category does not significantly impact the results. One can notice that CAM4 is more sensitive to the cloud scheme changes than is CSIRO-Mk3L. While both models have identical turbulence schemes, CSIRO-Mk3L has no shallow convection scheme. Hence, the larger sensitivity of CAM4 to the cloud scheme may be related to an interaction with the representation of shallow convection.

A direct comparison between each simulation could require a careful retuning of the model. An advantage of fixed-SST experiments is that the perturbed model will at least have the same SST and thus a relatively similar climate. However, the impact of model changes on the atmospheric radiative budget, or the direct

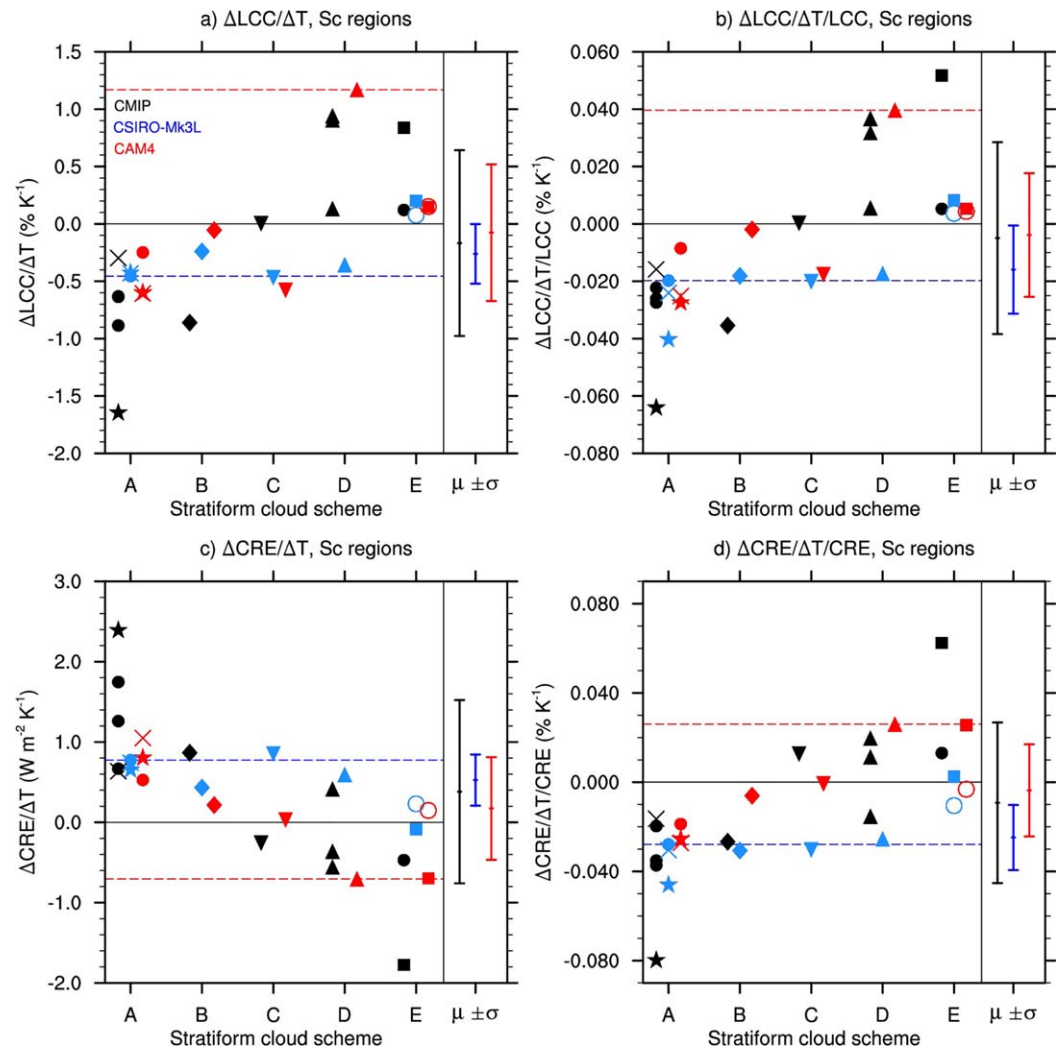


Figure 1. Response per unit of warming in the stratocumulus (Sc) regions for (a) cloud fraction, (b) normalized cloud fraction, (c) CRE, (d) normalized CRE (y axis), for the models summarized in Table 1, ranked per microphysical scheme type (x axis). The symbols also denote the type of cloud scheme used in the model: A (circle: A1, cross: A2, star: A3), B (diamond), C (downward triangle), D (upward triangle), E (square: E1, circle: E2). Black symbols denote CMIP models. Red and blue symbols denote simulations with CAM4 and CSIRO-Mk3L, respectively, in which the cloud schemes have been modified at low levels only (below 750 hPa), to match the corresponding scheme category. Note that cloud scheme E2 is not fully implemented and is represented by open circle. For both CAM4 and CSIRO-Mk3L, the default simulation with their original scheme is shown by a horizontal dashed line of the corresponding color. The right part of each plot shows the mean (μ) and two standard deviation (σ) of the CMIP, the CSIRO-Mk3L and the CAM4 ensemble.

effect of changes in mean-state cloud cover, could alter the cloud feedbacks. Indeed, modification of the cloud scheme involves some spreading of the range of LCC and CRE. The LCC and CRE within Sc regions of the modified models fall relatively within the range of CMIP models, with a tendency for CAM4 to be characterized by large LCC, with a mean bias of about 5% in comparison with the CMIP ensemble, and a tendency for CSIRO-Mk3L to be characterized by small LCC and small (in absolute value) CRE with mean biases of -4% and 9 W m^{-2} , respectively (supporting information Figure S1). By considering both CSIRO-Mk3L and CAM4 simulations together, no particular relationship is found between these variables in the mean cloud state and their response. In addition, the deployment of some cloud schemes (e.g., category B) changes the mean state CRE in opposite directions in CAM4 and CSIRO-Mk3L (supporting information Figure S1). However, the impact on LCC tends to have similar sign in both models. Retuning simulations would raise the question of which parameters to use for retuning, such as the parameters related to cloud radiative properties, or those of the cloud scheme, in particular for cloud schemes that have several parameters. Moreover, changing only the cloud scheme parameters may be not enough to impose a given CRE or LCC mean state.

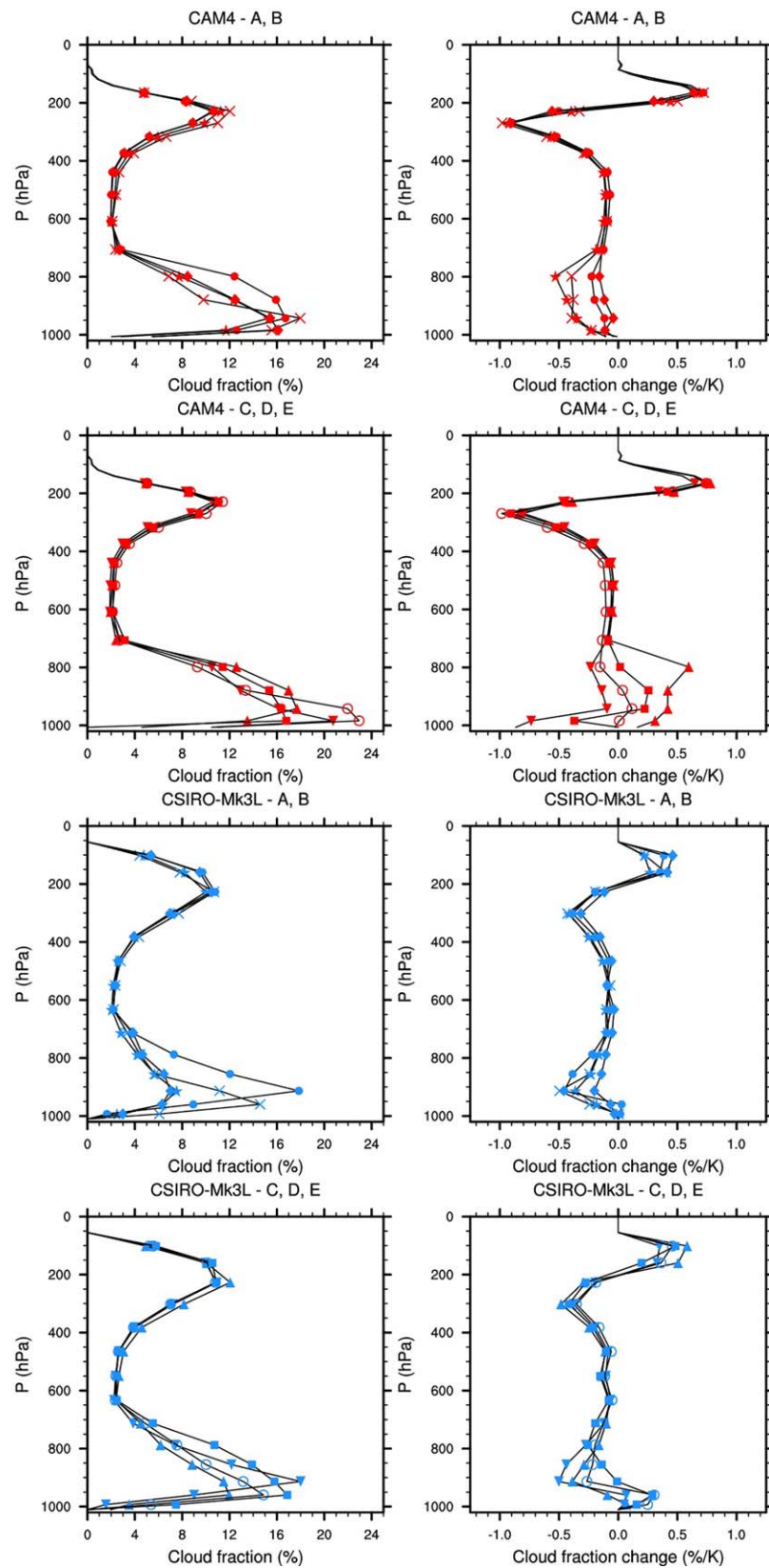


Figure 2. Mean vertical profile over the Sc regions of (left) cloud fraction and (right) cloud fraction change per unit of surface air warming for the category A-B scheme in CAM4 (first row), category C-E scheme in CAM4 (second row), category A-B scheme in CSIRO-Mk3L (third row), category C-E scheme in CSIRO-Mk3L (fourth row). Symbols are the same as in Figure 1.

Nonetheless, in order to partially remove effects associated with cloud changes in the mean state, we also show normalized change as done by *Webb et al.* [2015] for the CRE change (Figure 1c and 1d). Note however that focusing on normalized changes is not equivalent to retuning due to interactions between the cloud microphysics and macrophysics and their environment, at the process level. Moreover, normalization of the CRE responses is complicated by the masking offset between the CRE response and the cloud feedback [*Soden and Held, 2006*]. In the following, the behavior of each cloud scheme is discussed and responses are compared to CMIP models.

As shown in *Qu et al.* [2014], CMIP models with a PDF scheme are all characterized by a decrease in LCC in the Sc regions upon warming. This suggests a close link between the type of cloud scheme and the sign of the low cloud feedback in the Sc regions. The scheme-swapping results presented here confirm the robustness of this dependency (Figures 1a and 1b). In particular, implementation of any of the PDF schemes in CAM4 reverses the sign of the Sc-LCC change to a negative value, causing an increase of the (negative) Sc-CRE change. In PDF schemes, the cloud fraction can be expressed as a diagnostic function of RH alone. Putting aside feedback effects on RH changes associated with the cloud change itself [*Brient and Bony, 2012*], the behavior associated with PDF schemes suggests that climate models tend to predict a reduction in RH in subtropical regions in a warmer climate, leading to a reduction in cloud cover [e.g., *Sherwood et al., 2010*]. Apart from the dependency of cloud fraction to relative humidity, the role of cloud water content as predicted by these schemes would need to be investigated. However these changes are relatively moderate, suggesting the role of other important processes in imposing the magnitude of the cloud feedback.

The other scheme categories all involve dependence of the cloud fraction on other variables besides local humidity, in particular, stability. *Qu et al.* [2014] classify models based on the presence of such stability dependence of cloud fraction. They show that, except for models using *Scinocca et al.* [2008] parameterization (category B), CMIP models with stability dependence are characterized by an increase in cloud cover in Sc regions upon global warming. When the CAM4 Sc scheme is removed (not shown), the Sc-region LCC sensitivity becomes close to 0 ($\Delta CF/\Delta T_{as}=0.11\% K^{-1}$ without Sc scheme and $\Delta CF/\Delta T_{as}=1.16\% K^{-1}$ with Sc scheme) Hence, the CAM4 increase in Sc-region LCC upon warming is mainly due to the stability dependence of cloud fraction. However, the CRE response remains large without the Sc scheme, with a sensitivity $\Delta CRE/\Delta T$ of about $-0.71 W m^{-2} K^{-1}$ and $-0.22 W m^{-2} K^{-1}$ in the Sc regions, and $-0.60 W m^{-2} K^{-1}$ and $-0.47 W m^{-2} K^{-1}$ at global ocean scale, with and without Sc scheme, respectively (not shown). Hence the Sc scheme contributes to the low sensitivity of CAM4 but is not the main cause of it. When fitted with the CAM4 cloud scheme, CSIRO-Mk3L doesn't reproduce the large CRE increase seen in CAM4. Finally, these results show that a stability-sensitive Sc cloud scheme is not a sufficient condition for an LCC increase or large decrease in (negative) CRE.

The increase in LCC and decrease in CRE in the PCM (CCM3) model is reproduced by both CAM4 and CSIRO-Mk3L, when using the CCM3 cloud scheme (Figures 1a and 1c). When fitted with the CCM3 cloud scheme but without its Sc scheme component, the LCC change in CSIRO-Mk3L is roughly unchanged and the CRE change is even slightly smaller than with the CCM3 Sc scheme component, suggesting that the ω dependency of cloud fraction, and maybe also the diagnostic cloud water parameterization, play an important role in the low sensitivity of PCM.

Volodin [2014] attributes part the low climate sensitivity of INM-CM4 to the stability dependency of the cloud fraction formulation. In the present analysis, the INM-CM4 shows a very small Sc-region LCC changes (Figure 1a). With INM-CM4 cloud scheme, both CSIRO-Mk3L and CAM4 show a reduction in Sc-regions LCC. Thus, the stability dependency in INM-CM4 doesn't necessary lead to a LCC increase. However, the CRE change remains large, in particular for CAM4 (Figures 1c, 1d, 3a, and 3b). This is apparently due to a large optical depth feedback (not shown) associated with the increasing relationship between cloud water content and temperature [*Volodin, 2014*]. Hence the low sensitivity of INM-CM4 is likely to be due to its particular treatment of cloud water content rather than cloud cover.

Finally, the decrease in cloud cover for the *Scinocca et al.* [2008] cloud scheme (category B) is confirmed by CAM4 and CSIRO-Mk3L simulations (Figure 1a), but with a small magnitude for both models. The similarity to PDF schemes may be due to the fact that in this scheme stability plays a much weaker role compared to RH. Like PDF schemes, this scheme may tend to predict a positive feedback.

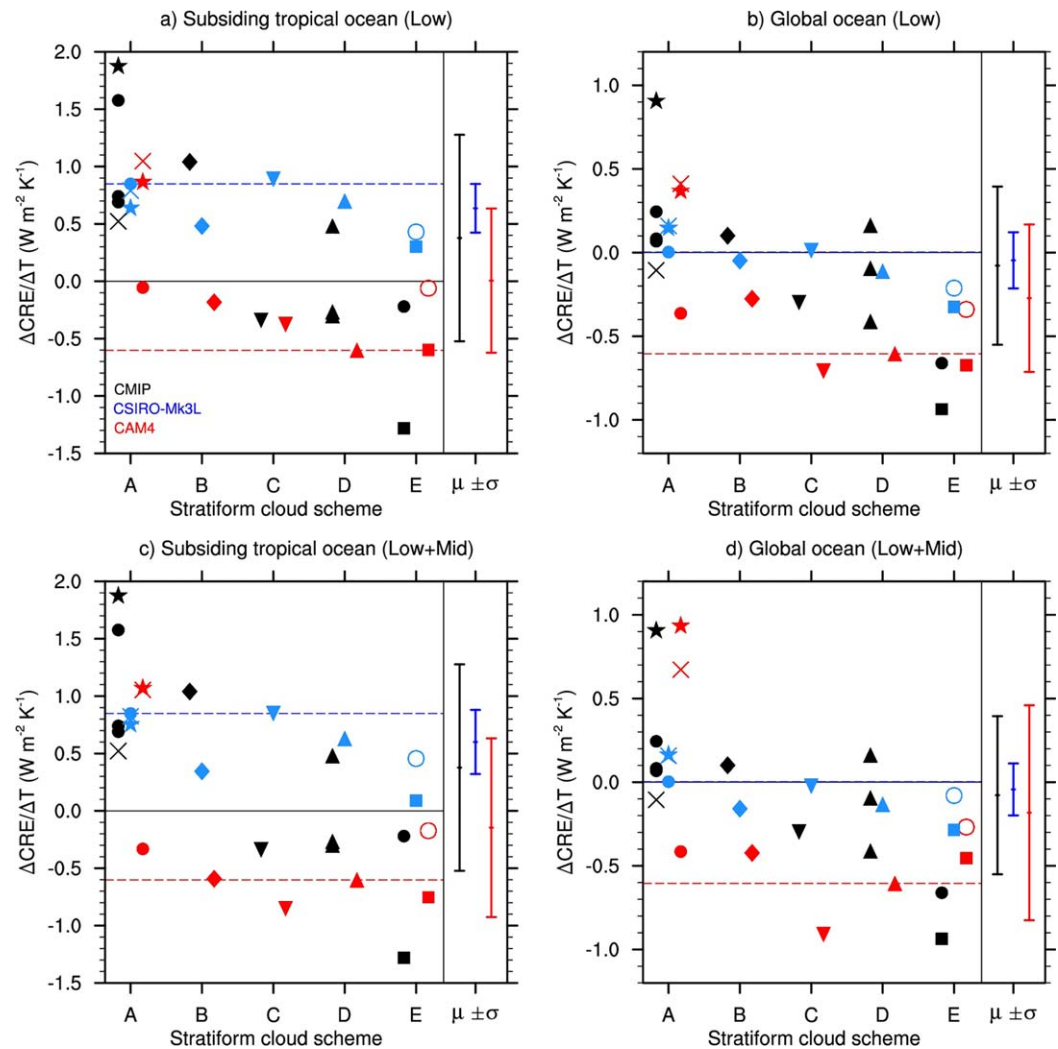


Figure 3. Same as Figure 1c, for the subsiding tropical ($30^{\circ}S-30^{\circ}N$) (left) ocean and (right) the global ocean, with cloud scheme modified only (top) at low levels and (bottom) at both low and midlevels.

3.2. Tropical and Global Scales

In the following, we focus on the responses at the tropical and global scales. Because of differences in experiment design used to determine LCC and CRE changes (uniform warming in fixed SST experiments or CO_2 increase in slab or coupled experiments), and potential differences in cloud parameters in some models over land, we focus on the responses over ocean only (tropical ocean is defined as the regions over ocean between $30^{\circ}S$ and $30^{\circ}N$). Note however that tests with the CSIRO-Mk3L have found results to be insensitive to whether or not the cloud scheme is modified over ocean only or over both ocean and land (not shown). For the tropics, we also focus on response in subsiding regions only, to avoid strong effects associated with deep convection.

The trends of the LCC response with scheme type in the two testbed climate models are similar in the subsiding tropical ocean, global ocean, and Sc regions (supporting information Figures S2a, S2b, S3a, and S3b). However, the CRE responses differ somewhat among the two testbed climate models and CMIP models in the subsiding tropical ocean (Figure 3a and supporting information Figure S2). Considering the whole tropical ocean, the spread in CRE responses is similar to that in subsiding regions only, but differences between the mean of each testbed model ensemble and the mean of CMIP subensemble CRE responses are enhanced by about a factor of two (not shown). The more unpredictable responses at the tropical scale compared to Sc regions may be due to an enhanced role of shallow convection, given that convection schemes are known to be able to influence cloud feedback. This may also be due to a role of deeper

convective events that affect CRE. The variations in tropical cloud feedback among cloud scheme within the same category, such as category A (e.g., Figure 3a and supporting information Figure S2a), also suggests interaction between the cloud scheme and other processes such as convective mixing. The vertical profile of the critical parameter may play a role in shaping such differences in cloud feedback.

At the global ocean scale (Figure 3b and supporting information Figure S3), the perturbed CAM4 and CSIRO-Mk3L experiments exhibit a large spread of sensitivities in comparison with the sub-CMIP ensemble, and with a relatively similar tendency for the feedback to decrease with ascending scheme category. The spread of CRE changes in CAM4 and CSIRO-Mk3L ensembles is about 93% and 35% of that of the sub-CMIP ensemble, respectively. These results suggest a substantial contribution of the stratiform cloud scheme to the inter-model spread in global cloud feedback. Note that the mean cloud fraction change at the global scale may be more difficult to interpret due to spatial heterogeneities in cloud regimes at global scale. However, as for the other scales, large differences are obtained between simulations with the two testbed models and corresponding CMIP models, for some schemes. In particular, the A category covers a large spread of sensitivities, with low sensitivity for the *Smith* [1990] scheme compared to the others PDF schemes. Lastly, in the extratropical ocean, the relationship between the cloud scheme and LCC response is similar to that of other regions (supporting information Figures S4a and S4b). However, the CMIP models do not exhibit such a relationship for the CRE (supporting information Figures S4c and S4d). This suggests an increasing role of other feedbacks than those related to low cloud fraction changes. Moreover, this suggests that the better agreement between the three model sets for global-average feedback than for that in subsiding tropical ocean regions may be partly due to compensating errors.

3.3. Cloud Scheme Changes at Both Low and Midlevels

In the experiments presented so far the cloud scheme was modified only below 750 hPa, but we have also extended the change to 300 hPa to include both low and midlevel cloud. Altitude 300 hPa was chosen because it corresponds to the default limit between midlevel and high level clouds in CAM4. Note that a separation at 440 hPa might be better as used by ISCCP cloud classification. In the Sc regions, the additional effect on the cloud responses is minor in comparison with effects via low levels only (not shown). At the tropical and global scale, including the deeper clouds tends to increase the spread in CRE changes (Figures 3c and 3d; supporting information Figures S5 and S6). Note that sensitivity to the cloud parameterization at levels above 300 hPa has not been investigated. Due to the FAT hypothesis [Hartmann and Larson, 2002] one can expect that larger quantities of cirrus would impact the feedback. Hence such simulation would necessitate a retuning of the high cloud fraction. Note that for some cloud schemes (B, C, and E1), the cloud scheme change significantly impacts the cloud fraction vertical profile, with high cloud (cirrus) cover peaking at about 300 hPa (supporting information Figure S7), which can be considered as unrealistic. For the Category B scheme, the normalized CRE change at the global scale (supporting information Figure S6d) is large in comparison with the simulation where the cloud scheme is modified only below 750 hPa, due to a very small CRE in the mean state (supporting information Figure S8b). This points to potential limitations in the strategy of normalizing CRE responses to control-state CRE amount, since the clouds responsible for the small CRE may differ from those responsible for the warming response.

4. Discussion and Conclusions

The stratiform cloud cover and cloud water content parameterizations used by a subset of CMIP models have been implemented in two testbed global atmospheric models, CAM4 and CSIRO-Mk3L. The schemes' impact on cloud responses to global warming, in terms of LCC and CRE, has been investigated using AMIP (specified SST) simulations, and responses have been compared to those of the CMIP models using the same cloud schemes. Note that some components of these cloud schemes have not been investigated, such as convective cloud and stratiform precipitation. Moreover, the impact of cloud scheme in high cloud regions (above 300 hPa) has also not been investigated.

The ensemble of cloud schemes tested is found to produce a substantial spread of cloud feedback in comparison to that of the full CMIP ensemble (about 40% and 65% of the CMIP subensemble for CRE changes in the Sc regions and global ocean, when varying the treatment of clouds below 750 hPa). Changing the cloud scheme can often reverse the sign of the feedback. These results suggest an important role of the cloud scheme in determining the cloud feedback of a climate model, showing in particular that cloud

feedback cannot be uniquely determined by characteristics of other schemes such as shallow convection or turbulence.

More specifically, PDF schemes and others [Scinocca *et al.*, 2008] where cloud cover is determined mainly by local relative humidity, tend to predict a decrease of low level cloud cover and an increase in (negative) CRE (hence a positive cloud radiative feedback) in Sc regions, confirming the results of Qu *et al.* [2014]. This may be explained by a tendency of climate models to reduce subtropical RH generally [Wetherald and Manabe, 1980; Sherwood *et al.*, 2010] in a warmer climate. However, a large spread is obtained for cloud schemes within the same category. These differences which can be due to relative differences in the vertical profile of the critical parameters or to differences in the underlying PDFs, highlight the equivalent importance of other boundary layer processes in imposing cloud feedback. In addition, at the scale of the tropics, results are less consistent, suggesting an important role of the coupling with other boundary layer parameterization in convective regions in determining the strength of the low cloud feedback. At the global ocean scale, the spread obtained in cloud responses is again closer to that obtained for the stratocumulus region, suggesting an important role of these cloud types (or the model schemes meant to represent them) for global cloud feedback.

Our results also suggest that particular cloud scheme assumptions may be sufficient, or at least necessary, to impose a negative sign of the low cloud feedback in the Sc regions. Stability dependence of cloud cover is found to play a major role in determining the LCC increase in CAM4 in the Sc regions. However, this stability dependence is not a sufficient condition for a cloud increase, as shown by the cloud reduction in CSIRO-Mk3L when fitted with this scheme. Note also that the effect of this scheme on the CRE response remains small, though not negligible, at the global scale. Hence the Sc scheme alone does not appear to explain the low sensitivity of CAM4. Similarly, in INM-CM4, the cloud water content parameterization appears to play an important role in explaining a low sensitivity, rather than stability dependency of the cloud fraction. Finally, other peculiarities of the cloud scheme, such as ω dependency, may play a determinant role in low sensitivities.

Some limitations can be pointed out. First, only two testbed models are used to perform these sensitivity experiments. Also, we did not attempt to retune the modified models, some of which may be out of radiative balance or have other mean-state errors larger than typical in CMIP (although it should be noted that CMIP5 models also have a fairly large range in mean state LCC and CRE). A second important caveat of this study is its limitation to a subset of the cloud schemes used by CMIP models. This subset represents roughly two thirds of climate models in the CMIP3 and CMIP5 ensemble. However, for practical reasons, it is biased toward the simplest cloud schemes. Investigating the role of prognostic cloud fraction schemes in the spread of cloud feedback, would be of particular interest but is more challenging.

Finally, our results confirm that the cloud scheme alone does not impose the feedback strength in a climate model, leaving a significant role for other parameterizations such as the schemes directly affecting shallow convection [e.g., Zhang *et al.*, 2013; Gettelman *et al.*, 2012; Sherwood *et al.*, 2014]. In this context, the fact that CSIRO-Mk3L is less sensitive to variations in the cloud scheme than is CAM4, may be primarily due to the lack of a shallow convection scheme in the CSIRO-Mk3L model. More generally, the impact of changing a cloud scheme may be sensitive to the alignment between the location where it predicts clouds and where other processes such as shallow convective mixing exert their strongest influence, rather than the formulation inherent to the cloud scheme itself. This suggests the importance of developing cloud schemes and other boundary layer parameterizations in a consistent way.

Appendix A: Stratiform Cloud Schemes Description and Implementations Details

A1. Category A

The A category encompasses schemes that assume a probability-density function (PDF) for the subgrid distribution of the moisture. These schemes are the most common type used in the CMIP3 and CMIP5 ensembles. The cloud fraction CF and the in-cloud water content q_{cl}^{in} read, respectively [Smith, 1990; Le Treut and Li, 1991; Bony and Emanuel, 2001]:

$$CF = \int_{q_c}^{\infty} P(q_t') dq_t'$$

$$q_{cd}^i = \int_{q_s}^{\infty} q_t' P(q_t') dq_t'$$

where P is the probability density function of the subgrid total water content q_t' and q_s is the saturation water vapor content. Note that in these schemes, the cloud fraction can equivalently be written as a function of RH only. The cloud water content is a function of RH and total water.

In the literature, schemes differ in particular in the assumed PDF. Here we consider three subclasses referred to as categories A1, A2 and A3:

1. Category A1 refers to the *Smith* [1990, hereinafter S90] scheme. The PDF is assumed to be a triangular function. The parameter of the scheme is a critical relative humidity RH_0 above which water vapor is assumed to condense. This parameter is set to CSIRO-Mk3L values ($RH_0 = \max(0.85, \sigma)$), where σ is the scaled pressure level. Note also that in the CSIRO-Mk3L, the threshold relative humidity varies in convective regions between cloud base and cloud top.
2. Category A2 refers to the *Le Treut and Li* [1991, hereinafter LL91] scheme. The PDF is assumed to be a uniform function. The parameter of the scheme, referred to as γ in LL91, is related the width of the distribution to the total water content. It is set to LL91 value ($\gamma = 0.2$).
3. Category A3 refers to the *Bony and Emanuel* [2001, hereinafter BE01] scheme (hereafter BE01). The PDF is assumed to be a Gaussian function. The parameter r_0 of the model relates the standard deviation of the distribution to the total water content. It is assumed to vary linearly with pressure between the surface and 300 hPa, with $r_0 = 0.95$ at surface and $r_0 = 0.33$ at 300 hPa, following *Hourdin et al.* [2006].

In S90 and LL91, the saturation water vapor content is diagnosed from the liquid temperature $T_l (= T - L_v q_{cd} - L_f q_{ice})$, where q_{ice} is ice water content and L_v and L_f are latent heat of vaporization and latent heat of fusion, respectively). In BE01, the saturation water vapor content is diagnosed from temperature.

In some climate model cloud schemes such as that of CSIRO-Mk3L, the cloud water content is a prognostic variable, following *Rotstayn* [1997], but the scheme remains a diagnostic scheme in the sense that cloud water is not used in the calculation of cloud variables.

A2. Category B

The B category refers to the scheme implemented in CGCM3 model and mainly described in *Scinocca et al.* [2008].

A2.1. Cloud Fraction

The cloud fraction reads:

$$CF = \widetilde{CF} (1 + \Lambda) / (1 + \widetilde{CF} \Lambda)$$

where

$$\widetilde{CF} = R \frac{R + \Lambda}{1 + \Lambda},$$

$$R = \begin{cases} \frac{RH - RH_0}{1 - RH_0} & , RH > RH_0 \\ 0 & , RH \leq RH_0 \end{cases}$$

and where the so-called conditional stability parameter Λ is given by:

$$\Lambda = \begin{cases} 0 & , \Gamma \leq \Gamma_s \\ \left(\frac{\Gamma - \Gamma_s}{\Gamma_s} \right)^2 & , \Gamma > \Gamma_s \end{cases}$$

where Γ is the local potential temperature lapse rate and Γ_s is the moist adiabatic lapse rate. The threshold relative humidity RH_0 is a function of the conditional stability parameter:

$$RH_0 = \frac{RH_0^1 + RH_0^2 \Lambda}{1 + \Lambda}$$

with $RH_0^1 = 0.95$ and $RH_0^2 = 0.87$ for liquid water and $RH_0 = 0.75$ for ice water.

A2.2. Cloud Water Content

The in-cloud water content is assumed to be proportional to the adiabatic water content of an air parcel lifted through a small vertical displacement, following *Betts and Harshvardhan* [1987] and *McFarlane et al.* [1992]:

$$q_{cld}^{in} = (C_p T / L_v \theta) \Gamma_s \rho_{air} g \Delta z$$

where g is gravity, ρ_{air} is density of dry air, $\Delta z = \min\left(150 \frac{(1+\Lambda)}{\Lambda}, \Delta z_{grid}\right)$ for liquid water and $\Delta z = \min(60, \Delta z_{grid})$ for ice water and Δz_{grid} is the depth of the grid box. In addition the ice water content is rescaled by $(1 + \widetilde{CF}\Lambda)/(1 + \Lambda)$ (note that in CGCM3, this rescaling is applied to the ice water path used in radiative calculation).

A3. Category C

The C category refers to the cloud scheme implemented in INM-CM4 model and described in *Volodin* [2014].

A3.1. Cloud Fraction

The cloud fraction is a linear function of RH with the parameters depending on local stability:

$$CF = a \cdot RH + b,$$

where a and b are set to values given by *Volodin* [2014] above ocean: $a=10$ and $b=-9$ for $\partial T/\partial z \geq -0.001$ K/m, $a=18.18$ and $b=-17.91$ for $\partial T/\partial z \leq -0.007$ K/m, and a and b are linear functions of $\partial T/\partial z$ for $-0.007 \leq \partial T/\partial z \leq -0.001$.

A3.2. Cloud Water Content

The in-cloud water content is expressed as a function of temperature:

$$q_{cld}^{in} = \frac{1}{1000 \rho_{air}} 10^{-1.03739 + 0.03130 \times (T - 273.15)}.$$

A4. Category D

The D category refer to the cloud scheme originally incorporated in CAM3 or CAM4, and described in *Neale et al.* [2010]. The CAM4 source code is available at <http://www.cesm.ucar.edu/models/ccsm4.0/cam/>.

A4.1. Cloud Fraction

Cloud fraction is expressed as the maximum of a cloud fraction depending on RH, CF_{RH} , and a cloud fraction given by a Sc scheme, CF_{Sc} :

$$CF_{RH} = \left(\frac{RH' - RH_0}{1 - RH_0} \right)^2,$$

where RH_0 is equal to 0.80 above 750 hPa, and to 0.91 and 0.81 below 750 hPa, over ocean and land, respectively. Note that the relative humidity is adjusted with the convective cloud fraction CF_{conv} : $RH' = RH(1 - CF_{conv}) / (1 - CF_{conv})$. The cloud fraction CF_{Sc} is given by a generalization of the scheme introduced by *Slingo* [1987] scheme and is expressed as a linear function of the lower tropospheric stability LTS and is bounded by the maximum of the relative humidity of the considered grid box and that of the underlying grid box $RH_{k,k-1}$:

$$CF_{Sc} = \min(0.057 \cdot LTS + 0.5573, RH_{k,k-1}).$$

The cloud is assumed to be located where the stability jump is the strongest and whether it exceeds 0.125 K hPa⁻¹.

A4.2. Cloud Water Content

The cloud water content follows a prognostic scheme from which a full description is provided in *Neale et al.* [2010]. The cloud water condensation/evaporation rate is written as a linear function of the rain evaporation rate, and the temperature, the water vapour and the cloud water tendencies, with the parameters depending on cloud fraction, thermodynamical variables, and in-cloud water content. For practical reasons, the term depending on the precipitation evaporation rate ($c_e E_r$ in equation (4.137) in *Neale et al.* [2010]) is neglected for implementation in CSIRO-Mk3L (note that no sensitivity has been found to this term for CAM4 simulations).

A5. Category E

A5.1. Cloud Fraction

The E1 category refers to the scheme of CCM3. It is described in *Kiehl et al.* [1996] and CCM3.6.16 source code is available at <http://www.cgd.ucar.edu/cms/ccm3/source.shtml>. Below 750 hPa, and if no stratocumulus is diagnosed, the cloud fraction is a function of both vertical velocity and relative humidity:

$$CF = \begin{cases} 0 & \omega \geq \omega_c \\ \frac{\omega_c - \omega}{\omega_c} \left(\frac{RH - RH_0}{1 - RH_0} \right)^2 & 0 \leq \omega < \omega_c \\ \left(\frac{RH - RH_0}{1 - RH_0} \right)^2 & \omega < 0 \end{cases} \quad (A1)$$

With $\omega_c = 50$ mb/d, and RH_0 equal to 0.90 and 0.80 over ocean and over land, respectively. Note that RH is used for implementation in CSIRO-Mk3L. Note that in CCM3 scheme, RH is an adjusted large scale relative humidity.

In addition, category E1 incorporates a Sc scheme following *Slingo* [1987]. Where $-d\theta/dp$ is maximum in the column boundary layer (below 750 hPa and above 900 hPa), and exceeds 0.125 K/hPa, the cloud fraction is expressed as a function of stability:

$$CF = \begin{cases} 0 & RH_{k-1} < 0.6 \\ \left(-6.67 \frac{\partial \theta}{\partial p} - 0.667 \right) \cdot \left(1 - \frac{0.9 - RH_{k-1}}{0.3} \right) \cdot \left(\frac{P - 750}{150} \right) & 0.6 \leq RH_{k-1} < 0.9 \\ \left(-6.67 \frac{\partial \theta}{\partial p} - 0.667 \right) \cdot \left(\frac{P - 750}{150} \right) & 0.9 \leq RH_{k-1} \end{cases}$$

where RH_{k-1} is relative humidity of the underlying grid box.

Above 750 hPa, cloud fraction follows:

$$CF = \left(\frac{RH - RH_0}{1 - RH_0} \right)^2$$

where RH_0 is expressed as a function of the square of the Brunt-Väisälä frequency N^2 :

$$RH_0 = 0.999 - 0.1 \left(1 - \frac{N^2}{3.5 \cdot 10^{-4}} \right)$$

Category E2 refers to the scheme implemented in FGOALS-s2 [*Bao et al.*, 2013]. The cloud fraction formulation follows equation (A1) [*Liu et al.*, 1998; *Bao et al.*, 2013], with $RH_0=0.85$ at low levels and $RH_0=0.78$ at midlevels (Q. Bao, personal communication, 2016). FGOALS-s2 also has a Sc scheme [*Fushan et al.*, 2005] that was not implemented in CSIRO-Mk3L and CAM4.

A5.2. Cloud Water Content

In CCM3 (category E1) the cloud water path used by the radiative transfer model is diagnosed from vertically integrated water vapor mixing ratio, while precipitation is diagnosed from a different formulation based on an "all or nothing" scheme assuming all condensed water precipitates. Here, the formulation used for the cloud water path, input to the radiative code, is also used to diagnose precipitation. Following this formulation, the cloud liquid water content reads [*Kiehl et al.*, 1996]:

$$q_{cl}^{in} = 250 \cdot 10^{-6} \frac{1}{\rho_{air}} h_l \left(e^{-\frac{z_{k-0.5}}{h_l}} - e^{-\frac{z_{k+0.5}}{h_l}} \right) / (z_{k+0.5} - z_{k-0.5}),$$

where $h_l = 700 \cdot \ln \left(1 + 1/g \int_{p_{top}}^{p_{surf}} q(p) dp \right)$ and $z_{k-0.5}$ and $z_{k+0.5}$ are the heights on the k^{th} layer interfaces.

In FGOALS-s2 (category E2) the cloud water content is formulated following *Xu and Randall* [1996]. Here it is written following equation (1) of *Xu and Randall* [1996]:

$$q_{cl}^{in} = -10^{-4} \ln \left(1 - \frac{CF}{RH^{0.5}} \right).$$

Acknowledgments

We thank two anonymous reviewers for their careful reading of the manuscript and their insightful comments and suggestions. We gratefully thank the NCAR Community Earth System Model team for making CAM4 and CCSM3 climate models code available. We thank S. Phipps for assistance concerning CSIRO-Mk3L climate model. We also thank the Canadian Centre for Climate Modelling and Analysis and Jason Cole for providing details of the cloud scheme of CGCM3 climate model, and Lijuan Li and Qing Bao, for information on FGOALS-s2 and FGOALS-g2 cloud schemes. Thanks are also due to Mark Webb, Andrew Gettelman, Alejandro Di Luca for discussions on this topic. We acknowledge the World Climate Research Programme's Working Group on Coupled Modelling, which is responsible for CMIP, and the U.S. Department of Energy's Program for Climate Model Diagnosis and Intercomparison which provides coordinating support and led development of software infrastructure in partnership with the Global Organization for Earth System Science Portals. We thank the climate modeling groups for producing and making available their model outputs. The CMIP data are available at http://cmip-pcmdi.llnl.gov/cmip5/data_portal.html. This work was supported by ARC grant DP140101104.

References

- Bao, Q., et al. (2013), The flexible global ocean-atmosphere-land system model, spectral version 2: FGOALS-s2, *Adv. Atmos. Sci.*, *30*(3), 561–576, doi:10.1007/s00376-012-2113-9.
- Bentsen, M., et al. (2012), The Norwegian earth system model, NorESM1-M-Part 1: Description and basic evaluation, *Geosci. Model Dev. Discuss.*, *5*, 2843–2931.
- Betts, A. K., and Harshvardhan (1987), Thermodynamic constraint on the cloud liquid water feedback in climate models, *J. Geophys. Res.*, *92*, 8483–8485, doi:10.1029/JD092iD07p08483.
- Bony S., and K. Emanuel (2001), A parameterization of the cloudiness associated with cumulus convection; evaluation using TOGA COARE data, *J. Atmos. Sci.*, *58*(21), 3158–3183.
- Bretherton, C. S. (2015), Insights into low-latitude cloud feedbacks from high-resolution models, *Philos. Trans. R. Soc. A*, *373*, 20140415. [Available at <http://dx.doi.org/10.1098/rsta.2014.0415>.]
- Bretherton, C. S., P. N. Blossey, and C. R. Jones (2013), Mechanisms of marine low cloud sensitivity to idealized climate perturbations: A single-LES exploration extending the CGILS cases, *J. Adv. Model. Earth Syst.*, *5*, 316–337, doi:10.1002/jame.20019.
- Brient, F., and S. Bony (2012), How may low-cloud radiative properties simulated in the current climate influence low-cloud feedbacks under global warming?, *Geophys. Res. Lett.*, *39*, L20807, doi:10.1029/2012GL053265.
- Chylek, P., J. Li, M. K. Dubey, M. Wang, and G. Lesins (2011), Observed and model simulated 20th century Arctic temperature variability: Canadian Earth System Model CanESM2, *Atmos. Chem. Phys. Discuss.*, *11*, 22,893–22,907.
- Collins, W. D., et al. (2004), Description of the NCAR community atmosphere model (CAM 3.0), *NCAR Tech. Note NCAR/TN-464+ STR*, 226 pp., Natl. Cent. for Atmos. Res., Boulder, Colo.
- Dufresne, J.-L., and S. Bony (2008), An assessment of the primary sources of spread of global warming estimates from coupled atmosphere-ocean models, *J. Atmos. Sci.*, *21*, 5135–5144.
- Dufresne, J. L., et al. (2013), Climate change projections using the IPSL-CM5 Earth System Model: From CMIP3 to CMIP5, *Clim. Dyn.*, *40*(9–10), 2123–2165.
- Fushan, D. A. I., Y. Rucong, X. Zhang, and Y. Yu (2005), A statistically-based low-level cloud scheme and its tentative application in a general circulation model, *Acta Meteorol. Sin.*, *19*(3), 263.
- Geoffroy, O., D.Saint-Martin, D.J. Ollivié, A. Voldoire, G. Bellon, and S. Tytéca (2013), Transient climate response in a two-layer energy-balance model. Part I: Analytical solution and parameter calibration using CMIP5 AOGCM experiments, *J. Clim.*, *26*, 1841–1857.
- Gettelman, A., J. E. Kay, and K. M. Shell (2012), The evolution of climate sensitivity and climate feedbacks in the community atmosphere model, *J. Clim.*, *25*, 1453–1469.
- Gordon, H. B. et al., (2002), The CSIRO Mk3 Climate System Model, *Tech. Pap. 60*, CSIRO Atmos. Res., Aspendale, Victoria, Australia. [Available at http://www.cmar.csiro.au/e-print/open/Gordon_2002a.pdf.]
- Gregory, D., and P. R. Rowntree (1990), A mass flux convection scheme with representation of cloud ensemble characteristics and stability dependent closure, *Mon. Weather Rev.*, *118*, 1483–1506.
- Gregory, J. M., W. J. Ingram, M. A. Palmer, G. S. Jones, P. A. Stott, R. B. Thorpe, J. A. Lowe, T. C. Johns, and K. D. Williams (2004), A new method for diagnosing radiative forcing and climate sensitivity, *Geophys. Res. Lett.*, *31*, L03205, doi:10.1029/2003GL018747.
- Hack, J. J. (1994), Parameterization of moist convection in the National Center for Atmospheric Research Community Climate Model (CCM2), *J. Geophys. Res.*, *99*, 5551–5568.
- Hartmann, D. L., and K. Larson (2002), An important constraint on tropical cloudclimate feedback, *Geophys. Res. Lett.*, *29*, 1951, doi:10.1029/2002GL015835.
- Holtstlag, A. A. M., and C.-H. Moeng (1991), Eddy diffusivity and countergradient transport in the convective atmospheric boundary layer, *J. Atmos. Sci.*, *48*, 1690–1698.
- Hourdin, F., et al. (2006), The LMDZ4 general circulation model: Climate performance and sensitivity to parametrized physics with emphasis on tropical convection, *Clim. Dyn.*, *27*, 787–813, doi:10.1007/s00382-006-0158-0.
- Kiehl, J. T., J. J. Hack, G. B. Bonan, B. A. Boville, B. P. Briegleb, D. L. Williamson, and P. J. Rasch (1996), Description of the NCAR Community Climate Model (CCM3), *NCAR Tech. Note NCAR/TN-420+STR*, Natl. Cent. for Atmos. Res., Boulder, Colo. doi:10.5065/D6FF3Q99.
- Le Treut, H., and Z.-X. Li (1991), Sensitivity of an atmospheric general circulation model to prescribed SST changes: Feedback effects associated with the simulation of cloud optical properties, *Clim. Dyn.*, *5*, 175–187.
- Li, L., et al. (2013), The flexible global ocean-atmosphere-land system model, Grid-point Version 2: FGOALS-g2, *Adv. Atmos. Sci.*, *30*, 543–560.
- Liu, H., X. Zhang, and G. Wu (1998), Cloud feedback on SST variability in the western equatorial Pacific in GOALS/LASG model, *Adv. Atmos. Sci.*, *15*(3), 412–423.
- Martin, G. M., et al. (2011), The HadGEM2 family of Met Office Unified Model climate configurations, *Geosci. Model Dev.*, *4*, 723–757, doi:10.5194/gmd-4-723-2011.
- McFarlane, N. A., G. J. Boer, J.-P. Blanchet, and M. Lazare (1992), The Canadian Climate Centre second-generation general circulation model and its equilibrium climate, *J. Clim.*, *5*, 1013–1044.
- Meehl, G. A., C. Covey, and K. E. Taylor (2007), The WCRP CMIP3 multimodel dataset: A new era in climate change research, *Bull. Am. Meteorol. Soc.*, *88*, 1383–1394.
- Neale, R. B., et al. (2010), Description of the NCAR community atmosphere model (CAM 4.0), technical report, NCAR, Natl. Cent. for Atmos. Res., Boulder, Colo.
- Phipps, S. J., L. D. Rotstayn, H. B. Gordon, J. L. Roberts, A.C. Hirst, and W. F. Budd (2011), The CSIRO-Mk3L climate system model version 1.0 – Part 1: Description and evaluation, *Geosci. Model Dev.*, *4*, 483–509.
- Qu X., A. Hall, S. A. Klein, and P. M. Caldwell (2014), On the spread of changes in marine low cloud cover in climate model simulations of the 21st century, *Clim. Dyn.*, *42*(9–10), 2603–2626.
- Rieck M., L. Nuijens, and B. Stevens (2012), Marine boundary layer cloud feedbacks in a constant relative humidity atmosphere, *J. Atmos. Sci.*, *69*(8), 2538–2550.
- Ringer, M. A., T. Andrews, and M. J. Webb (2014), Global-mean radiative feedbacks and forcing in atmosphere-only and coupled atmosphere-ocean climate change experiments, *Geophys. Res. Lett.*, *41*, 4035–4042, doi:10.1002/2014GL060347.
- Rotstayn, L. D. (1997), A physically based scheme for the treatment of stratiform clouds and precipitation in large-scale models, I: Description and evaluation of the microphysical processes, *Q. J. R. Meteorol. Soc.*, *123*, 1227–1282, doi:10.1002/qj.49712354106.
- Rotstayn, L. D., M. A. Collier, M. R. Dix, Y. Feng, H. B. Gordon, S. P. O'Farrell, I. N. Smith, and J. Syktus (2010), Improved simulation of Australian climate and ENSO-related rainfall variability in a global climate model with an interactive aerosol treatment, *Int. J. Climatol.*, *30*(7), 1067–1088.

- Scinocca, J. F., N. A. McFarlane, M. Lazare, J. Li, and D. Plummer (2008), Technical Note: The CCCma third generation AGCM and its extension into the middle atmosphere, *Atmos. Chem. Phys.*, *8*, 7055–7074, doi:10.5194/acp-8-7055-2008.
- Sherwood, S. C., W. Ingram, Y. Tsushima, M. Satoh, M. Roberts, P. L. Vidale, and P. A. O’Gorman (2010), Relative humidity changes in a warmer climate, *J. Geophys. Res.*, *115*, D09104, doi:10.1029/2009JD012585.
- Sherwood, S. C., S. Bony, and J. Dufresne (2014), Spread in model climate sensitivity traced to atmospheric convective mixing, *Nature*, *505*, 37–42.
- Slingo, J. M. (1987), The development and verification of a cloud prediction scheme for the ECMWF model, *Q. J. R. Meteorol. Soc.*, *113*, 899–927.
- Smith, R. N. B. (1990), A scheme for predicting layer clouds and their water content in a general circulation model, *Q. J. R. Meteorol. Soc.*, *116*, 435–460.
- Soden, B. J., and I. M. Held (2006), An assessment of climate feedbacks in coupled ocean-atmosphere models, *J. Clim.*, *19*, 3354–3360.
- Stainforth, D. A., et al. (2005), Uncertainty in predictions of the climate response to rising levels of greenhouse gases, *Nature*, *433*, 403–406.
- Taylor, K. E., Ronald, J. Stouffer, and G. A. Meehl (2012), An overview of CMIP5 and the experiment design, *Bull. Am. Meteorol. Soc.*, *93*(4), 485–498.
- Volodin, E. M. (2014), Possible reasons for low climate-model sensitivity to increased carbon dioxide concentrations, *Izv. Atmos. Oceanic Phys.*, *50*(4), 350–355.
- Volodin, E. M., N. A. Dianskii, and A. V. Gusev (2010), Simulating present-day climate with the INMCM4.0 coupled model of the atmospheric and oceanic general circulations, *Izv. Atmos. Oceanic Phys.*, *46*(4), 414–431.
- Washington, W. M., et al. (2000), Parallel climate model (PCM) control and transient simulations, *Clim. Dyn.*, *16*(10–11), 755–774.
- Watanabe, S., et al. (2011), MIROC-ESM: Model description and basic results of CMIP5-20c3m experiments, *Geosci. Model Dev. Discuss.*, *4*(2), 1063–1128.
- Webb, M. J., et al. (2015), The impact of parametrized convection on cloud feedback, *Philos. Trans. R. Soc. A*, *373*, 2054.
- Wetherald, R. T., and S. Manabe (1980), Cloud cover and climate sensitivity, *J. Atmos. Sci.*, *37*, 1485–1510.
- Wu, T., R. Yu, F. Zhang, Z. Wang, M. Dong, L. Wang, X. Jin, D. Chen, and L. Li (2010), The Beijing Climate Center atmospheric general circulation model: Description and its performance for the present-day climate, *Clim. Dyn.*, *34*(1), 123–147.
- Xu, K. M., and D. A. Randall (1996), A semiempirical cloudiness parameterization for use in climate models, *J. Atmos. Sci.*, *53*(21), 3084–3102.
- Zelinka, M. D., C. Zhou, and S. A. Klein (2016), Insights from a refined decomposition of cloud feedbacks, *Geophys. Res. Lett.*, *43*, 9259–9269, doi:10.1002/2016GL069917.
- Zhang, G. J., and N. A. McFarlane (1995), Sensitivity of climate simulations to the parameterization of cumulus convection in the Canadian Climate Centre general circulation model, *Atmosphere-Ocean*, *33*, 407–446.
- Zhang, M., et al. (2013), CGILS: Results from the first phase of an international project to understand the physical mechanisms of low cloud feedbacks in single column models, *J. Adv. Model. Earth Syst.*, *5*, 826–842, doi:10.1002/2013MS000246.
- Zhao, M., et al. (2016), Uncertainty in model climate sensitivity traced to representations of cumulus precipitation microphysics, *J. Clim.*, *29*(2), 543–560.